

Scaling of the Background Brain Dynamics and Alpha Rhythm

D. C. Lin¹, A. Sharif¹, H. C. Kwan²¹Department of Mechanical and Industrial Engineering,

Ryerson University, Toronto, Ontario, Canada

²Department of Physiology, University of Toronto, Toronto, Ontario, Canada

(Dated: December 23, 2021)

Abstract

The scaling property of the brain dynamics is studied based on the zero-crossing of the local electroencephalographic (EEG) recording taken from healthy young adults in eyes closed and eyes open. Evidence of coupling between the EEG fractal dynamics and the α rhythm is presented. An organization principle that governs this coupling relationship is proposed. In the dominant brain state, a possible interpretation using the self-organized criticality similar to the punctuated equilibrium is discussed.

PACS numbers: 87.19.Hh, 87.10.+e

I. INTRODUCTION

The cortical activity of the human brain in wakefulness and eyes-closed typically exhibits the 8–12 Hz rhythm¹. Although its origin remains open^{2;3}, this classical rhythm has been associated with the "resting" state of the cortex with most pronounced activity recorded in the parietal and occipital areas.

While the rhythm represents one of the major cortical activities, there typically lies a background "noise" component of unknown functionality and origin⁴. There is growing evidence of the importance of this background component. For example, local surface scalp measurements based on electroencephalography^{4;5;6;7} (EEG) and magnetoencephalography⁸ reveal its fractal characteristics coexisting with moderate rhythm. Similar results were found in multi-channel recording^{4;6;7;8}, suggesting the global nature of the fractal dynamics in the cortex. The relevance of this background fluctuation in physiology may be seen from its state dependence property^{8;22} where normal individuals in eyes closed average to a larger scaling exponent than in eyes open. Recent works further imply that the EEG fluctuation may have a broader implication on the other autonomic function such as the cardiovascular regulation^{9;10}.

The purpose of this study is to investigate the EEG background fluctuation and its coexistence with the rhythm. While they are separately subjects of intense study, far less understood is the organization of these two prominent features of the brain dynamics. In addition, the findings reviewed above may require further clarifications when the oscillation becomes dominant. For example, a trained meditator or Yoga practitioner can shift a significant portion of the EEG signal power to the band that obscures any potential fractal characteristics in the background fluctuation. Fig. 1 shows EEG's with moderate and strong rhythm from a normal subject and an experienced Yoga practitioner, respectively. It is observed that the power law trend diminishes almost entirely in the dominant EEG, but not in the moderate EEG. This apparently inverse relationship with the strength of rhythm implies either the fractal background fluctuation is buried in the oscillation, and can thus no longer be detected from the amplitude characteristics of the EEG, or there is simply no long-range correlated fluctuation in the dominant brain state. Using the detrend fluctuation analysis¹¹ (DFA) on the integrated dominant EEG actually supports the latter scenario of a white noise process in the background fluctuation (DFA exponent = 0.5); see Fig. 1c. However, as we show below, it is not a valid description for the dominant brain

state.

In this work, we use the zero-crossing property to study the EEG background fluctuation coexisting with rhythm. EEG zero-crossing has been primarily used to extract event-related frequency information¹². Despite the obvious advantage of being insensitive to amplitude artefacts, the use of zero-crossing to study EEG background fluctuation appears scarce. Watters and Martins used DFA to analyze the "EEG walk" constructed from the zero-crossing of EEG showing moderate rhythm¹³. These authors found evidence of scaling and rejected the (uncorrelated) random-walk interpretation for the EEG background component. But we should point out that a DFA scaling exponent 0.5 (random walk) is in fact possible in the dominant brain state (Fig. 1c).

By excluding the wave zero-crossing, we will show that the EEG background does exhibit fractal characteristics. For the scaling analysis in dominant case, the zero-crossing approach is found to be more effective than other amplitude-based methods such as the power spectral density function and DFA. The complementary set of the background zero-crossing in the real line captures other EEG activities. For the dominant case, this complementary set describes mainly the dynamics. With the combined EEG fractal background, we conjecture fractal scaling in the emergence of dynamics. Support to this conjecture is found in the power law distribution of the interval. Our analysis also suggests that the dominant brain state may be interpreted in the universality class of the self-organized criticality¹⁵ of punctuated equilibrium¹⁴. While SOC has been proposed for the EEG fluctuation in the frequency band^{7,8}, and its analytical phase⁴, our result provides further evidence of its possible connection to the organization of the EEG background dynamics and the rhythm. Finally, we are able to write down the governing principle for this organization that relates the EEG fractal scaling and the emergence of dynamics.

In the next section, the main idea of extracting the zero-crossing of EEG background fluctuation is described and verified with artificial examples. In section III, the method is applied to the EEG records taken from subjects showing little to significant rhythm. Discussion and concluding remarks are given in the last section.

II. METHODS AND NUMERICAL EXAMPLES

A. Main Ideas

Let the EEG be $x(t)$. The zero-crossing time is the level set $t_i; x(t_i) = 0$ where the index i registers the order of the zero crossing event. In practice, t_i is first determined by linear interpolation and then used to define the set of crossing-time-interval (CTI) $C = \{t_i = t_{i+1} - t_i\}$.

Zero-crossing of a stochastic process is a surprisingly hard problem; see, e.g., Ref. 16. Thanks to its self-similarity, the CTI for a fractal process is known to follow a power law distribution¹⁷: $p(\tau) \sim \tau^{-\alpha}$, where $p(\tau)$ is the probability density function (PDF). For example, $\alpha = 2 - h$ for the fractional Brownian motion (fBm) $B_h(t)$ of Hurst exponent h .

If fractal exists in the dominant EEG, it can be captured in CnA where A denotes the CTI of the oscillation. However, fractal CTI's can occasionally lie in the rhythm range¹⁸. It is thus not possible to obtain A based solely on the value of CTI.

What is characteristic to the rhythmic oscillation in general is a steady zero-crossing pattern of the oscillation. Hence, a set of CTI's is considered of origin if they correspond to continuous zero-crossing in the rhythm range. Specifically, we consider a bigger set A using the following two criteria: (i) the CTI lies in the range of rhythm range and (ii) the CTI's are from continuous zero-crossing. Let such CTI's be denoted by

$$A_i = [t_i; t_{i+1}; \dots; t_{i+m_i}]; \quad (1a)$$

$m_i > 1; i = 1; 2; \dots$. This describes the i^{th} event segment in the EEG record. The CTI's for the dynamics is estimated by the union of A_i 's:

$$A = \{A_i\}; \quad (1b)$$

Inevitably, some continuous zero-crossing could still come from the potential fractal component of the EEG. Hence, A is only a subset of A . The "error" $A \setminus A$ depends on the fractal property as well as the strength of the rhythm. The complement CnA captures irregular zero-crossing that is characteristic to the fractal process.

For moderate oscillation, EEG may contain other rhythmic components. The check of continuous zero-crossing must then be extended to a reasonably large scale range. To this end, we first consider the set of large CTI fluctuation: $I_1 = \{t_i > \tau_u \text{ or } t_i < \tau_l\}$ where $\tau_u; \tau_l$

are the upper and lower thresholds for defining the set of large CTI. Let K denote the CTI's from continuous zero-crossings in $(CnI_1) \cap A$ and let $I_0 = (CnI_1) \cap (K \cup A)$. Finally, the set of fractal CTI is obtained by

$$F = I_1 \cup I_0 \quad (1c)$$

Note that this definition does not preclude fractal crossing in the δ rhythm range. Note, for the dominant case, that continuous crossing is mainly captured in A and, thus, $K \subset f;g$ and we recover $F \subset CnA$ as shown above. If $\mu = \langle \mu \rangle - 1$, where $\langle \mu \rangle$ is the mean of $f;g$, any accidental fractal crossing included in $K \cup A$ will not introduce bias to the power law distribution of the fractal crossing (Fig. 2 below).

B. Numerical Examples

To demonstrate the above idea, we used Hilbert transform to construct the fractal time series given by the amplitude process of fBm, $A_h(t)$. This is to mimic the fractal property reported in the band-passed EEG⁷. Note that $A_h(t)$ inherits the same scaling characteristics from $B_h(t)$. Hence, $h = 2 - \mu$ holds, where μ is estimated from the histogram of CnA . To define A , $\mu = \exp(-5)$ and $\mu = \exp(-1)$ were used. These values are determined from the range of CTI of $A_h(t)$: $\mu = 0.8 \max(C)$, $\mu = t$, the sampling time. Fig. 2 shows the PDF estimate of CnA . It is seen that theoretical values are verified before and after deleting A (Fig. 2). This should be the case since no band-limited component exists in $A_h(t)$. It thus establishes deleting A defined above does not affect the power law PDF of a pure fractal signal.

To examine the influence from the band-limited rhythmic oscillation, $A_h(t)$ in randomly selected time intervals of variable length were replaced by a narrow-band process $x(t) = M(t)N(t)$ where $M = 1 + A_h(t)$ models the fractal amplitude modulation⁷ and the narrow-band $N(t)$ is a sine wave of Gaussian amplitude X and frequency f ; i.e., $X = N(1; \sigma_x)$ and $f = N(10; \sigma_f)$. Note that $N(t)$ has a 10-Hz central frequency to mimic the δ rhythm. To simulate the dominance of the band-limited oscillation, the probability of an interval being selected for $x(t)$ is four times of those for $A_h(t)$. In addition, the interval length for $x(t)$ is at least three times shorter than those for $A_h(t)$. The synthetic data so constructed is shown in Fig. 3a.

In presenting our results, we keep the time unit in all figures so as to make easy reference to the narrow-band oscillation. Segments of CTI's before and after deleting A are shown in

Figs. 3b, 3c. The corresponding $p(\cdot)$ are estimated in Fig. 3d. It is clear that the narrow-band component x can create significant bias in the otherwise power law PDF of $A_h(t)$. The theoretical power law $p(\cdot)$ for $A_h(t)$ is correctly described after deleting A defined by (1).

III. EEG SCALING AND THE ALPHA DYNAMICS

A. Scaling of the EEG Background Fluctuation

We now apply the zero-crossing method to EEG records with varying degrees of α rhythm. These records were collected from six subjects (3 males, 3 females) of age 21 to 30 year-old (mean: 24) who gave written consent to participate in the study. All subjects were instructed to maintain normal daily activity before participating in the 5-minute recording session. Surface scalp electrodes were attached according to the 10-20 international system at O1, O2, referencing to Cz. Two groups of data were taken: one in eyes open (EO) and one in eyes closed (EC). For EO, subjects were asked to direct their gaze at certain part of a shielded room to minimize eye movements. For EC, no specific instruction was given to the subjects other than to relax and have their eyes closed. Output impedance from the recording system has been kept below 5k Ω . The EEG was first band-passed from 0.1 to 70 Hz and then digitized with a 12-bit A/D precision at 250 Hz (first four subjects) and 500 Hz (last two subjects).

In order to measure the strength of the α rhythm, we use the ratio of EEG signal power in the 8–12 Hz band to the full accessible frequency range, $R = \frac{R_{12}}{8} S(f)df = \frac{R}{8} S(f)df$ (Fig. 4a). As expected, the R is larger in EC than in EO due to the lack of visual stimulation in EC. Three of the six subjects (S2, S3, S4) are able to generate dominant α rhythm with large R measure (> 0.45) in EC. It is important to note that low R measure could mean very little α activity; e.g., the corresponding power spectra are given by power law with little identifiable feature in the α band. In contrast, there is always a very distinct “peak” located at the 10 Hz range for subjects showing large R .

The CTIPDF's of all EEG data sets are found to be of the power law form $p(\cdot)$. This indicates the fractal dynamics continues to exist in the brain state showing α rhythm. In particular, qualitatively different $p(\cdot)$'s are found before and after deleting A from subjects showing dominant α rhythm (Fig. 4b), and almost the same $p(\cdot)$ from subjects showing

moderate to little rhythm (Fig. 4c, also Fig. 2). For estimating the scaling in dominant brain state, this means a more effective approach of using EEG zero-crossing than other amplitude-based methods such as the power spectrum and DFA (see also Fig. 1).

Similar to the literature⁸, state dependence of the EEG fractal is observed: the exponent is larger in EO than in EC. In addition, α and R follows an inverse relation in both EC and EO (Fig. 5a). If one tentatively compares to the Hurst model using $h = 2 - \alpha$, this result means a positive correlation between the EEG fractal background scaling and the underlying rhythm.

B. Alpha Interval and Organization of Complex Brain Dynamics

The inverse relationship shown in Fig. 5a further suggests a relationship between the scaling property of the EEG fractal background and the dynamics.

Consider first the zero-crossing points of the EEG fractal background in the real line: $I_F = \{t_1; t_2; \dots\}$ where t_i locates the end points of the CTI defined in F. The set I_F can be obtained by intersecting the fractal portion of the EEG graph X_F with the zero axis. Let \dim_{I_F} be the box-counting dimension for I_F . It is known from geometry that $\dim_{X_F} + 1 - 2 = \dim_{I_F}$ where the '1' on the left-hand-side of this equation is the dimension of the zero axis. By the Holder condition of the fractal function¹⁹, one can show $\dim_{X_F} \leq 2 - (2 - \alpha) = \alpha$. Thus, $\dim_{I_F} \geq 1$.

Similarly, one can define the zero-crossing points of the dynamics. In principle, this is obtained by intersecting the portion of the oscillation in the EEG graph with the zero axis. In practice, we use the A_i 's in (1a) to approximate the interval $L_i = \bigcup_{k=l_i}^{p_{m_i}} t_k$ where the L_i measures the "size" of the i^{th} event as it emerges in the foreground of the EEG. Unlike the l_i in (1a), which is narrowly distributed in the rhythm range¹⁸, L_i can in general cover a much wider range of values. The end points locating the intervals define the zero-crossing points $I_A = \{t_1; t_2; \dots\}$ g.

Given the EEG fractal background established in the last section, we conjecture the same for the interval and a power law PDF $p(L) \sim L^{-\alpha}$. Denote the box-counting dimension of I_A by \dim_{I_A} ; i.e., $n(T) \sim T^{\dim_{I_A}}$ where $n(T)$ is the number of zero-crossing points over the period T . The power law exponent can be connected to \dim_{I_A} via the relation¹⁴: $n(T) = T^{-\dim_{I_A}} \int_0^T p(L) L dL$ where $\int_0^T p(L) L dL$ on the right-hand-side estimates the average length of all intervals over the period T . Substituting the power law $p(L) \sim L^{-\alpha}$

yields $\dim_{I_A} = 1$.

Since the point sets I_F and I_A are embedded in the (1D) real line (time axis) and $I_F \setminus I_A = \emptyset$, one has

$$0 = \dim_{I_F} + \dim_{I_A} - 1 = (1) + (1) - 1 = 1.$$

Hence, we have the inequality that connects the power law exponents of the EEG fractal background and the length of the rhythm:

$$\alpha + \beta \geq 3. \quad (3)$$

Due to the little rhythm in our EO data sets, the estimation of $p(L)$ was suffered from poor statistics. For the EC data sets, both power law $p(L)$ and (3) are verified (Fig. 5b). We will thus focus only on the EC data in this section. In Fig. 5c, an interesting transition is shown from the inequality (3) in moderate cases (S1, S5, S6) to almost equality $\alpha + \beta = 3$ in dominant cases (S2, S3, S4). For $\alpha + \beta = 3$ (dominant) the numerical values 1.25 and 1.75 are estimated. For $\alpha + \beta > 3$ (moderate), larger α and β are estimated.

The case of 1.75 in the dominant EEG worths further discussion. In their model study of multi-trait evolution¹⁴, Boettcher and Paczuski (BP) predicted that evolution is a self-organized critical (SOC) process consisting of quiescent periods of all sizes, interspersed by short intervals of mutation event. These authors derived a similar power law scaling exponent of 1.75 for the distribution of the quiescent period and pointed out that their multi-trait model belongs to a new universality class. This universality condition prompted us to make the comparison of these two different phenomenologies. With the estimated 1.75, it is tempting to compare the interval with the quiescent period in the BP model. This leads to the hypothesis of SOC dynamics in the "resting" state of the cortex.

IV. DISCUSSION AND CONCLUSION

The EEG background fluctuation coexisting with varying degrees of rhythm is studied. It is important to note that our results directly address these two prominent features of the brain dynamics, rather than the EEG fluctuation in the frequency band^{7,8}. Compared to other amplitude-based methods, we show that zero-crossing is more effective for studying the scaling in dominant EEG.

Our main result is the evidence and characterization of the coupling between the EEG background fluctuation and the rhythm. Our findings can be summarized in two points:

(a) An inverse relationship between the EEG background scaling and the strength of rhythm is observed, with a larger exponent in EO for all subjects. Using the Hurst model tentatively ($h = 2$), this implies a larger scaling exponent in EC compared to EO, or the trend towards more anti-persistent fluctuation in the dominant brain state in EO.

Similar state dependence property has been reported in the past^{3;8}. Stam and de Bruin⁸ found similar result based on the correlation between the band desynchronization and the decrease of the (DFA) scaling exponent in EO. An inverse relation was also reported by Moosmanns et al.³ based on the blood oxygenation level dependence contrast as a measure of the brain metabolic activity. These authors concluded a dominant rhythm associated with metabolic deactivation and desynchronization, a view may further be supported by the increase of local cortical activity²⁰ and information processing during EO²¹.

(b) The inequality (3) characterizes the organization of the coupling. Since it is arrived based solely on the set-theoretic arguments, it is plausible that similar equations may exist between the EEG fractal background and other brain rhythms such as the α , β , γ waves.

The observed transition from $h > 3$ to $h \approx 3$ in dominant EEG, and the coincidence with the BP dynamics, imply a SOC state in the dominant EEG. Hence, a strong rhythm and the corresponding background fluctuation may represent two perspectives of the same dynamics. In general, this observation is in agreement with the suggestion of SOC of the EEG fractal dynamics^{4;7;8}. However, our result differs in that we find indication of SOC only at the dominant brain state, based mainly on the universality of the BP dynamics. For subjects showing little to moderate rhythm, the universality condition is no longer matched. We are not able to determine if a different universality class may be involved in these cases, nor can we ascertain a different theory for the observed fractal dynamics. Further studies on a larger population size and different physiological states are necessary to provide answers for these questions. They are the future work currently underway.

Acknowledgment

The authors would like to acknowledge supports from Natural Science and Engineering Research Council of Canada.

Reference

[1] H. Berger, *Arch Psychiat Nervenkr*, 87, 52 (1929); E.D. Adrian and B.H. Matthews, *Brain*, 57 355 (1934).

- [2] T. Inouye, K. Shinosaki, A. Yagasaki, A. Shimizu, *Clin. Neurophysiol*, 63, 353 (1986); P.L. Nunez, B.M. Wingerter, R.B. Silberstein, *Human Brain Mapping*, 13, 125 (2001).
- [3] M. Moosmann, P. Ritter, I. Krestel, A. Brink, S. Thees, F. Blankenburg, B. Taskin, H. Obrig, A. Villringer, *Neuroimage*, 20, 145 (2003); R. Goldmann, J.M. Stem, J. Engel Jr., M.S. Cohen, *Neuroreport*, 13, 2487 (2002).
- [4] W.J. Freeman, *Clin Neurophysiol* 115, 2089-2107 (2004).
- [5] P.A. Watters, *Int J Syst Sci*, 31, 819 (2000).
- [6] R. Hwa and T. Ferrel, *Phys Rev E*, 66, 021901 (2002);
- [7] C.J. Stam, E.A. de Bruin, *Human Brain Mapping*, 22, 97 (2004).
- [8] K. Linkenkaer-Hansen, V.V. Nikulin, J.M. Palva, K. Kaila, R.J. Timonen, *J Neurosci*, 15, 1370 (2001).
- [9] T. Murata, T. Takahashi, T. Hamada, M. Omori, H. Kosaka, H. Yoshida, Y. Wada, *Neuropsychobiol*, 50, 189 (2004).
- [10] see; e.g., H. Otzenberger, C. Simon, C. Groner, G. Brandenberger, *Neurosci Lett*, 229, 173 (1997); J. Ehrhart, M. Toussaint, C. Simon, C. Groner, R. Luthringer, G. Brandenberger, *Sleep*, 111, 940 (2000).
- [11] C.-K. Peng, S. Havlin, H.E. Stanley, A.L. Goldberger, *Chaos*, 5, 82 (1995).
- [12] J. Gaillard, *Neuropsychobiol*. 14, 210 (1987); B. Elizabeth et al., *Sleep Res Online*, 3, 113 (2000); R.M. Rangayyan, *Biomedical Signal analysis*, Wiley-IEEE Press (2001).
- [13] P.A. Watters and F. Martin, *Biol Psych*, 66, 79 (2004).
- [14] S. Maslov, M. Pacuski, P. Bak, *Phys Rev Lett* 74, 2162 (1994); M. Pacuski, P. Bak, S. Maslov, *Phys Rev Lett* 74, 4253 (1995); S. Boettcher and M. Pacuski, *Phys Rev Lett* 76, 348 (1996).
- [15] H.J. Jensen, *Self-Organized Criticality*, Cambridge Univ. Press, Cambridge (1998).
- [16] S.O. Rice, *Bell Syst Tech J*, 24, 46 (1945); B. Derrida, V. Hakim, R. Zeitak, *Phys Rev Lett*, 77, 2871 (1996).
- [17] M. Ding, W. Yang, *Phys Rev E*, 52, 207 (1995).
- [18] The wave crosses the zero axis twice per cycle. Assuming the mean frequency 10 Hz, the CTI is 1/10/2 second.
- [19] See Prop. 4.2 in K. Falconer, *Fractal Geometry*, John Wiley & Sons, New York (1995). For B_m , it is possible to achieve equality using potential theoretic approach and the Gaussian distribution of the increment.
- [20] G. Pfurtscheller and A. Aranibar, *Electroenceph Clin Neurophysiol*, 42, 817 (1997).

[21] C.J. Stam, M. Breakspear, A.M. Van Cappellen van Walsum, B.W. van Dijk, Human Brain Mapping, 19, 63 (2003).

Figure Caption

Fig. 1 (a) EEG records with moderate (top) and strong (bottom) rhythm, and the corresponding (b) power spectral density functions and (c) the DFA result¹¹ $F(l)$. The results for moderate (strong) rhythm are the top (bottom) curves in (b) and (c). They correspond to, respectively, subjects S4 and S5 in eyes closed (Fig. 4). The solid line in (b) marks the frequency 10 Hz ($\log(10) = 2.3$). The solid lines in (c) have the slopes 1.21 and 0.51, respectively.

Fig. 2 (a) An example of the CTI of $A_h(t)$, $h = 0.3$. (b) Log-log plot of $p(\cdot)$ for $A_{0.3}(t)$ (top) and $A_{0.8}(t)$ (bottom) before (open circles) and after (crosses) deleting A (see (1)). The axes are arbitrary. The solid lines are drawn with the theoretical slope 1.2 ($= 0.8 - 2$) and 1.7 ($= 0.3 - 2$). The filled circles describe the zero-crossing PDF of a gaussian white noise, where no power law can be claimed¹³.

Fig. 3 (a) A segment of the synthetic EEG. Two fractal periods are highlighted by horizontal bars in 161.5 – 162.5. (b) A segment of the set C . Note the concentration of i 0.05 sec. (c) The set $C \cap A$ where A is defined by (1). The horizontal lines mark the levels of $u \exp(-2.5)$ and $l \exp(-5)$. (d) Log-log plot of $p(\cdot)$ before (connected dots) and after (heavy solid line) deleting A . The light solid line has the theoretic slope, -1.9, from the fractal component in synthetic data ($A_{0.1}(t)$). The vertical line marks the 10 Hz oscillation¹⁸ ($\tau = 1/20$; $\log(\tau) = 2.9$).

Fig. 4 (a) The R measure for the six subjects. (b) Log-log plot of $p(\cdot)$ for subject S4 in EC showing dominant rhythm. A segment of the EEG for this subject has been shown in Fig. 1a. (c) Log-log plot of $p(\cdot)$ for a subject in EO showing little rhythm (S6 in (a)). The close (open) circles show the $p(\cdot)$ before (after) deleting A and the solid lines are the regression lines ($l \exp(-5)$ and $u \exp(-1)$).

Fig. 5 (a) The inverse relationship between τ and R in EO (open circles) and EC (solid circles). The subject index (used in Fig. 4) is given next to the symbol. (b) Log-log plots of $p(\cdot)$ and $p(l)$ for subjects showing dominant rhythm in EC: S2 (in asterik and circle, resp.), S3 (in plus and triangle, resp.), S4 (in cross and square, resp.). Solid lines with slopes -1.25 and -1.75 are drawn. (c) The plot of τ (solid circle), τ (open square) and $\tau + \tau$ (cross) for subjects in EC. R in Fig. 4a is reproduced and referenced to the left y-axis.

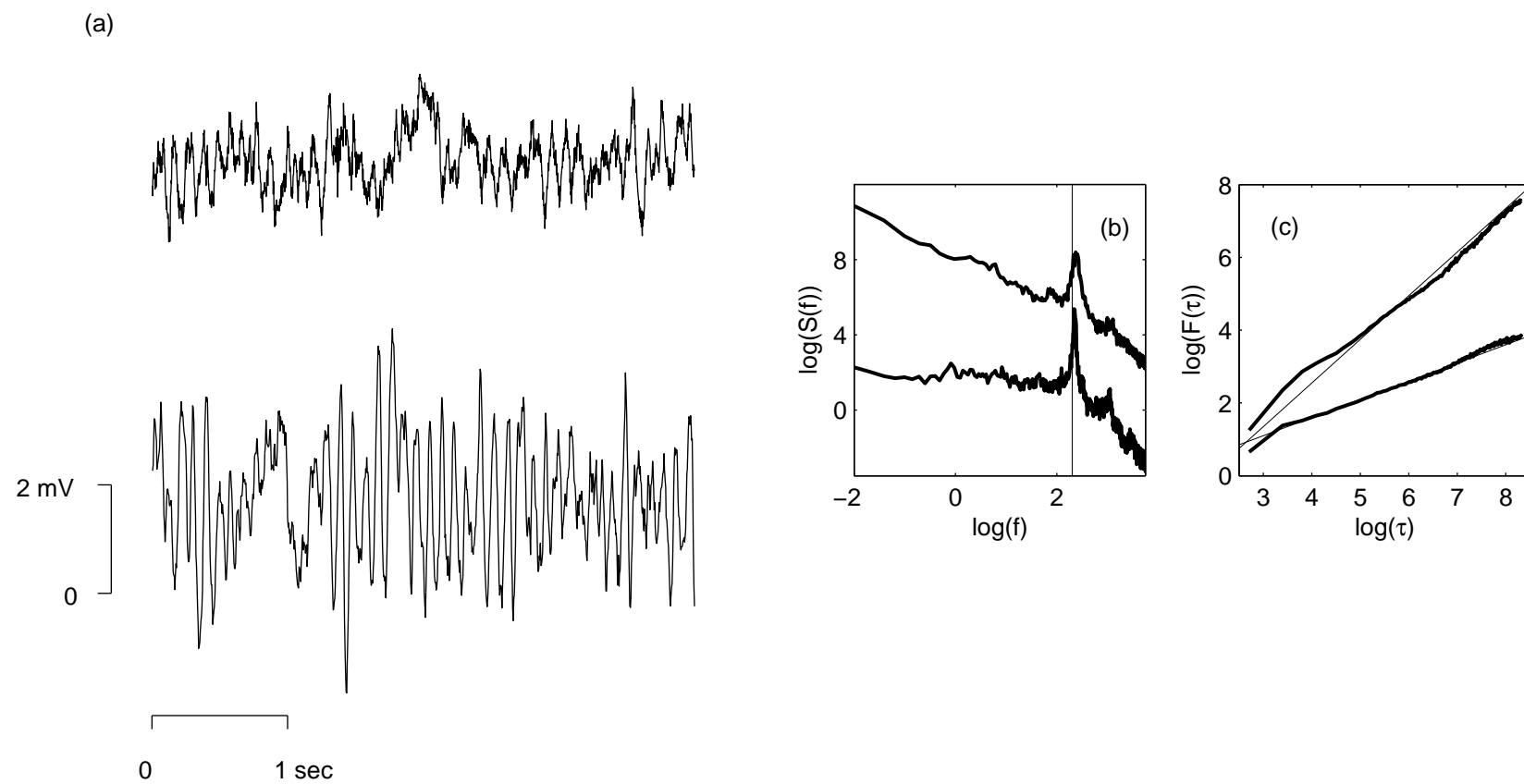


Figure 1

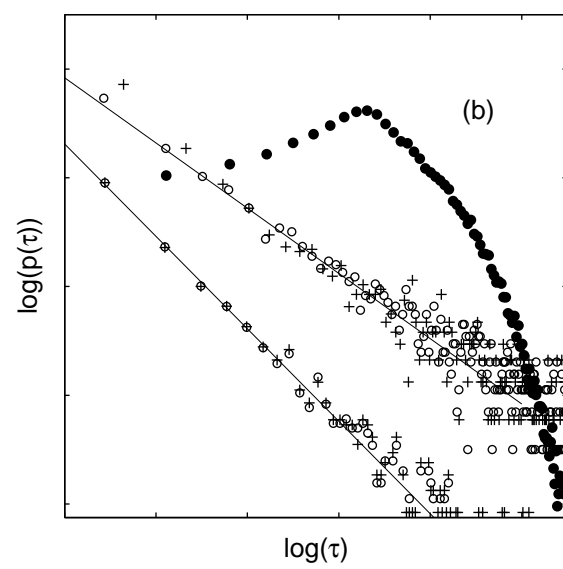
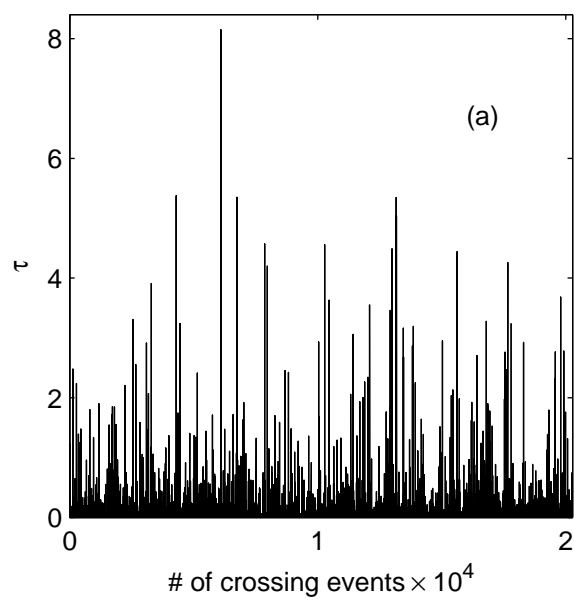


Figure 2

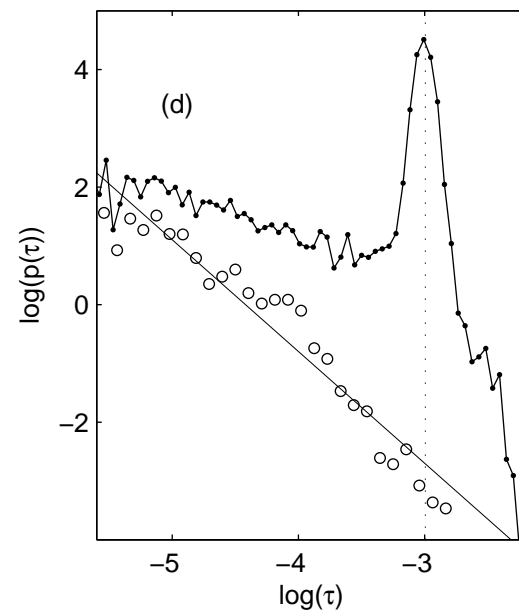
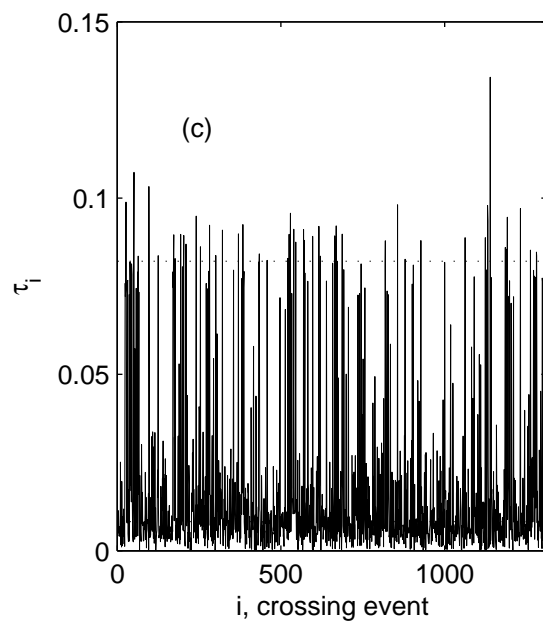
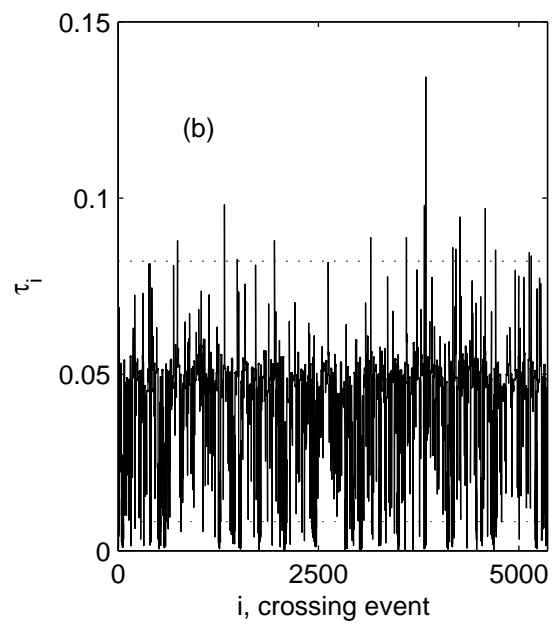
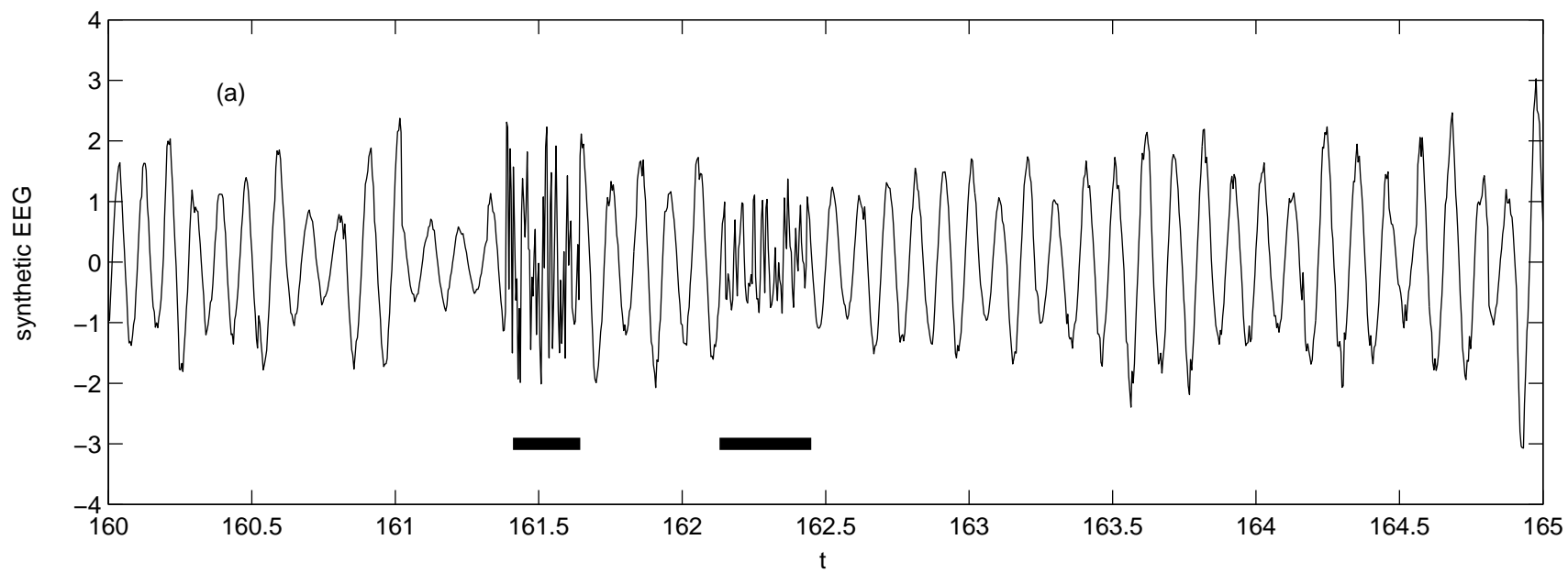


Figure 3

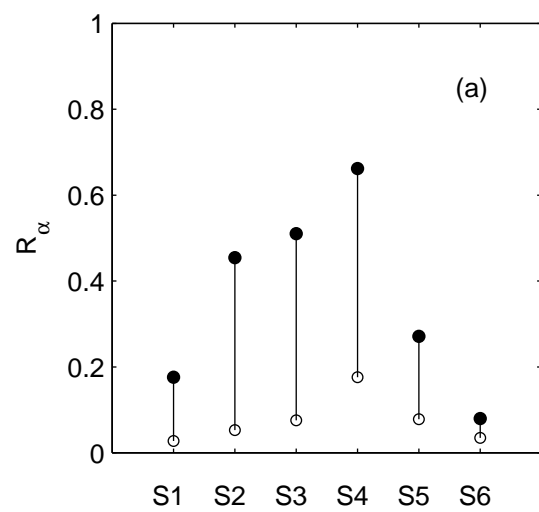


Figure 4

